Clays and Clay Minerals, Vol. 24, pp. 1–23. Pergamon Press 1976. Printedi n Great Britain

MORPHOLOGY OF ZEOLITES IN SEDIMENTARY ROCKS BY SCANNING ELECTRON MICROSCOPY

FREDERICK A. MUMPTON
Department of the Earth Sciences, State University College, Brockport, NY 14420, U.S.A.

and

W. CLAYTON ORMSBY
Office of Research, Federal Highway Administration, Washington, DC 20590, U.S.A.

(*Received* 3 *November* 1975)

Abstract—In the nearly 2000 occurrences of zeolites in sedimentary rocks of volcanic origin about 15 zeolite minerals have been identified. The mode of occurrence of six of these, clinoptilolite, erionite, chabazite, phillipsite, analcime, and mordenite, is described, and their morphology is illustrated with scanning electron micrographs.

INTRODUCTION

Although zeolites have been known since 1756 as minor constituents in vugs and cavities of basalts and other mafic igneous rocks, they have just recently emerged from the dusty drawers of mineral collections to be recognized as one of the most abundant and significant silicates in sedimentary rocks. No longer mere mineralogical curiosities, zeolites are now mineral commodities in the true sense of the word. Nearly 2000 occurrences have been reported since the late 1950s in sedimentary rocks of volcanic origin in more than 40 countries. Their intriguing adsorption, ion-exchange, catalytic and dehydration properties are the basis for dozens of commercial applications in many areas of industrial and agricultural technology, and more than 300 000 tons of zeolitic tuff are mined each year and used in the paper industry, in pozzolanic cements and concrete, as lightweight aggregate, in fertilizer and soil conditioners, as ion exchangers in pollution-abatement processes, as dietary supplements in animal husbandry, in the separation of oxygen and nitrogen from air and as acid-resistant adsorbents in gas drying and purification (Mumpton, 1975).

Most sedimentary occurrences of zeolite minerals are in rocks of Cenozoic age. They are thought to have formed chiefly by the alteration of volcanic glass in aqueous environments, shortly after deposition. Such deposits are generally flat-lying and range in thickness from less than a centimeter to more than 100 meters. Several distinct types of deposits are recognized including (1) deposits formed from pyroclastic materials in "closed" saline-lake basins, (2) deposits formed in "open", freshwater lake or groundwater systems, (3) deposits formed in true marine environments, (4) deposits formed by low-grade, burial metamorphism, (5) deposits formed by hydrothermal or hot-spring activity, (6) deposits formed from volcanic debris or clay minerals in alkaline soils, and (7) deposits formed without direct evidence of volcanic precursors (Mumpton, 1973a; Sheppard, 1973; Munson and Sheppard, 1974). About 15 different zeolites have been identified in sedimentary rocks; however, analcime, chabazite, clinoptilolite, erionite, heulandite, laumontite, mordenite, and phillipsite are the most common, with clinoptilolite ranking "number one" in abundance.

Many zeolitic sedimentary rocks are quite pure and beds containing up to 95% of a single species are common. Generally two or more zeolites are present as well-formed, micron-size crystals, along with varying amounts of fresh volcanic ash, cristobalite, montmorillonite, potassium feldspar, and other authigenic minerals. Minor amounts of pyrogenic and detrital quartz, feldspar, mica, etc. are also present but are commonly much coarser grained. The very small particle size of authigenic zeolites makes their examination by ordinary light microscopy extremely difficult. Normal transmission electron microscopy also yields less than satisfactory results, especially if information on the textural relationships of co-existing phases is desired. The ease of sample preparation and the great depth of field obtainable by *scanning electron microscopy* combine to make S.E.M. an ideal technique for the examination of sedimentary zeolite assemblages. The form, habit, size, and spatial relationships of constituent minerals can easily be observed *without* disrupting the aggregate. S.E.M. data are also useful from the point of view of understanding growth mechanisms which may have been responsible for the transformation of volcanic glass to euhedral zeolite crystals (Mumpton, 1973b). The textures of such assemblages are also of considerable value, for example in the development of beneficiation processes for commercial deposits.

EXPERIMENTAL

Using a Cambridge Stereoscan model S-4 scanning electron microscope, the morphological characteristics of the most important sedimentary zeolites listed above were determined from as many genetically different types of deposit as possible. More than 100 specimens were examined in this investigation and nearly 500 photographs taken; however, only a few illustrating the common morphologies of these zeolites are shown. Samples were broken to expose fresh surfaces, and chips about 2–10 mm in size were cemented with silver paste to half-inch diameter aluminum discs and dried at about 55°C in a vacuum oven. The samples were then coated with a composite film of carbon (100 Å) and gold–palladium alloy (200 Å) to insure electrical conductivity and thus prevent charging effects in the microscope. Images generated by the emission of secondary electrons were examined on the phosphorescent screen of the instrument and photographed with a polaroid camera. Selected areas also were examined by non-dispersive X-ray spectroscopy using a detector and analyzer manufactured by EDAX Instrumental, Inc. to obtain qualitative elemental analyses of individual crystals.

DESCRIPTION OF ZEOLITES

Clinoptilolite

Clinoptilolite in sedimentary rocks generally occurs as euhedral plates and laths, several micron in length and 1–2 microns thick. Most crystals display characteristic monoclinic symmetry, and many are coffin-shaped, mimicking megascopic heulandite that occurs in vugs and cavities of basalt. Typical assemblages of coarse-grained clinoptilolite are shown in Figs. 1 and 2, scanning electron micrographs of a lacustrine tuff from Castle Creek, Idaho, that was probably zeolitized under freshwater conditions. X-ray powder diffraction studies indicate that this sample is almost pure clinoptilolite; however, several thin scales of probable montmorillonite (see Borst and Keller, 1969) are in the fields of view. Similar clinoptilolite plates are shown in Fig. 3, a micrograph of a sample from the well-known locality at Hector, California (Ames, Sand and Goldich, 1958). Here, thin threads of a second phase lie atop and criss-cross the clinoptilolite plates. As discussed below, this material is mordenite, a zeolite that is easily recognized in X-ray diffraction patterns of Hector ore. Similar fibrous mordenite has been observed in most of the clinoptilolite samples examined in this study.

Clinoptilolite from Toponica, Yugoslavia, is much narrower and resembles laths rather than plates or blades. As seen in Fig. 4, it occurs in clusters of closely spaced, well-oriented crystals. Filiform mordenite is also present. The susceptibility of many sedimentary zeolites to changes in pore-water composition is illustrated by the severely etched clinoptilolite from Hungry Valley, Nevada, shown in Fig. 5. The ragged appearance of the crystals is probably due to partial dissolution after the zeolite formed from parent volcanic glass. The hole or pit in the large, coffin-shaped crystal in Fig. 6 may also be due to a secondary dissolution process.

In general, the monoclinic habit of clinoptilolite is easily recognized in the scanning electron microscope; however, many specimens contain masses of anhedral particles which, from X-ray powder diffraction analyses, must be clinoptilolite; however, these particles cannot be identified on the basis of morphology alone.

Erionite

Until about 1958, erionite was a rare mineral, found as woolly masses in only one locality near Durkee, Oregon. A scanning electron micrograph of the type material (Fig. 7) shows it to consist of closely packed fibers, wherein even the thinnest fiber seems to consist of even thinner members. The many sedimentary erionites examined in this study contain not what could be termed fibers, but rather clusters of acicular needles, as illustrated in Figs. 8 and 9. Most of the needles in Fig. 8, a micrograph of an erionite-rich tuff from a saline-lake deposit near Eastgate, Nevada, are 10–20 μm in length and 1–3 μm thick. The splintery nature of erionite needles is readily seen in Fig. 9, a micrograph of a similar tuff from Jersey Valley, Nevada. Note the "whisk-broom" manner by which needles split apart at their ends. A large fragment of volcanic glass is also shown in this figure. The pitted nature of the glass shard probably is due to arrested pore-water dissolution, and the absence of crystal growth on the surface of the residual glass fragment suggests a simple dissolution–precipitation mechanism for the formation of the zeolites in this sample (Mumpton, 1973b).

Figure 10 is a reproduction of Fig. 4 in Waltinger and Zirkl (1974) of megascopic erionite from a basalt cavity. The needles are several hundred microns in length and are characterized by hexagonal symmetry. The same hexagonal form is displayed by rods of sedimentary erionite from Shoshone, California, shown in Fig. 11 and seems characteristic of this phase. A somewhat different morphology is shown by erionite from a tuff collected near Hector, California (Figs. 12 and 13). Here bean-shaped bundles of needles are common. Each bundle is about 20 μm in length and about 10 μm thick and consists of hundreds of individual needles, each slightly less than a micron thick. A similar habit for erionite is shown in Fig. 14, a micrograph of an erionite–chabazite assemblage from Bowie, Arizona. Note the sheaf of erionite needles embracing another, both within a small cavity lined with micron-size crystals of chabazite.

Chabazite

Sedimentary chabazite generally occurs as cube-

https://doi.org/10.1346/CCMN.1976.0240101 Published online by Cambridge University Press

like rhombohedra, as illustrated in Figs. 15–19. Intergrown "cubes" or "rhombs", varying in size from less than a micron to several microns are not uncommon and are shown in Figs. 15 and 16, respectively. Isolated crystals up to 5 or 10 μm on a side also can be found (see Figs. 17 and 18). The cube-like habit is well developed in samples from both saline-lake and marine environments and, as pointed out in an earlier publication (Mumpton, 1973a), is similar to that displayed by chabazite in most of the world's traprock bodies; only the scale is different. Pore-water dissolution is again suggested by the mottled appearance of the chabazite rhombs shown in Fig. 19, a micrograph of a saline-lake tuff from Reese River Valley, Nevada.

Phillipsite

Although phillipsite is a common constituent of many sedimentary zeolite deposits, beds of the pure mineral are rare and have been found in only a few localities of the world. It occurs as stout prisms and stubby laths, 3–30 μm in length and 0.3–3 μm thick, as shown in Figs. 20–24. The pseudo orthorhombic symmetry is generally evident, especially where the crystals are capped by two-sided "domes", as illustrated in Fig. 21. A common characteristic of many phillipsites is a "cracking" along cleavage surfaces parallel to the axis of elongation, breaking the crystal into smaller sections (see Fig. 22). Phillipsite from saline-lake deposits also seems mottled or etched, also probably due to partial dissolution in response to changing pore-water composition. Rosettes or bundles of radiating crystals, as illustrated in Figs. 20 and 24, respectively, are not uncommon habits for this phase.

Analcime

Analcime is easily recognized in the scanning electron microscope by its characteristic cubo-octahedral and trapezohedral habits, as shown in Figs. 25–30. Figures 25 and 26 are micrographs of a marine tuff from Ischia, Italy. Euhedral crystals of 10–30 μm in diameter are common. Crystals of similar size and intergrowths of crystals in a green, saline-lake tuff from Wikieup, Arizona (Sheppard and Gude, 1973) are somewhat less well-developed and are coated with submicron-size flakes of a probable ferruginous clay mineral and/or potassium feldspar. (see Figs. 27 and 28) The cubic habit of sedimentary analcime is recognizable even in subhedral fragments or in crystals that are partially coated with montmorillonite, as illustrated in Figs. 29 and 30, micrographs of analcime-rich tuffs from lacustrine deposits near Barstow, California, and Tejupan, Mexico, respectively.

Mordenite

As mentioned above, mordenite is a constituent of almost every specimen of clinoptilolite-rich tuff examined in this study. It occurs as thin, curved fibers, a few tenths of a micron in diameter, coating grains and bridging gaps between larger grains of the platy zeolite. (See Figs. 3, 4, 5, 31 and 32.) The fibers are extremely delicate and length:width ratios of 100 or more are common. The filaments commonly intertwine into closely packed mesh structures (Fig. 33) and commonly form "rats' nests" of the type shown in Fig. 34, an electron micrograph of monomineralic mordenite from an ash-flow tuff near Beatty, Nevada. Coarser grained mordenite is the major constituent of a marine tuff from Pismo Beach, California and is shown in Fig. 35. The mordenite is needle-like and about 1 μm in diameter. A monomineralic tuff from a saline-lake deposit near Lovelock, Nevada, also contains relatively thick mordenite needles, arranged in radiate clusters (see Fig. 36).

A major problem plaguing the recognition of mordenite and erionite with the scanning electron microscope is the occurrence of both in the form of thin needles. If there is enough of either zeolite to be detected by X-ray powder diffraction, one can be reasonably confident of identification inasmuch as the two zeolites rarely occur together. If only trace amounts are present, the problem becomes difficult, and it may not be possible to distinguish these two zeolites, especially where the fibers are in the 1 μm-thick range. Thinner fibers have been observed only in mordenite samples, but thicker fibers are invariably erionite and may display characteristic hexagonal symmetry. By way of illustration, Fig. 37 is a scanning electron micrograph of a clinoptilolite-rich tuff from a large deposit in Dzegvi, Georgian S.S.R. described by Gvakhariya and others (1972). Neither erionite nor mordenite was reported in this deposit, nor can either zeolite be detected in X-ray diffraction patterns of the sample. Fibers from 0.5 to 0.8 μm in diameter, however, are plainly visible in the sample but cannot be identified unequivocally from the data available. If the fibers are erionite, this is the first occurrence of erionite to be recognized in sedimentary zeolite deposits of the U.S.S.R. Hopefully, further examination of zeolite samples from this deposit will resolve this question.

Acknowledgments—The authors are grateful to the Research Foundation of the State University of New York for early support of this project (Grant No. 228600A-6) and to the Office of Research, Federal Highway Administration for making its facilities available for this study. Thanks are also due to R. A. Sheppard, G. V. Gvakhariya and E. Passaglia for providing samples, and to R. A. Sheppard for having reviewed the manuscript.

REFERENCES

Ames, L. L., Jr., Sand, L. B. and Goldich, S. S. (1958) A contribution to the Hector, California bentonite deposit: *Econ. Geol.* **53,** 22–37.

Borst, R. L. and Keller, W. D. (1969) Scanning electron micrographs of API reference clay minerals and other selected samples: *Proc. Int. Clay Conf., Tokyo,* 1969 Vol. I.

Gvakhariya, G. V., Skhirtladze, N. I. and Batiashvili, T. V. (1972) Clinoptilolite-bearing volcanic tuff of the north slope of the Trialet Range: *Doklady Akad. Nauk, S.S.S.R.* **205,** 179–80.

Mumpton, F. A. (1973a) Worldwide deposits and utilization of sedimentary zeolites: *Industrial Minerals* (London) No. 73, 30–45.

Mumpton, F. A. (1973b) Scanning electron microscopy and the origin of sedimentary zeolites: Molecular Sieves: *Proc. 3rd Int. Molecular Sieve Conf.*, 159–161.

Mumpton, F. A. (1975) Commercial uses of natural zeolites: Section of 4th Edition of *Industrial Minerals and Rocks* (Edited by S. J. Lefond) pp. 1262–1274. *Am. Inst. Min. Metall. Petrol. Engrs.*

Munson, R. A. and Sheppard, R. A. (1974) Natural zeolites: their properties, occurrences, and uses: *Min. Sci. & Engng* **6,** 19–34.

Sheppard, R. A. (1973) Zeolites in sedimentary rocks: *U.S. Geol. Surv. Prof. Pap.* **820,** 689–95.

Sheppard, R. A. and Gude, A. J.,I II (1973) Zeolites and associated authigenic silicate minerals in tuffaceous rocks of the Big Sandy Formation, Mohave County, Arizona: *U.S. Geol. Surv. Prof. Pap.* **830,** 36 pp.

Waltinger, H. and Zirkl, E. J. (1974) Rasterelektronenmikroskopische Aufnahmen von Erionit aus Kollnitz, Lavanttal, Kärnten: *Carinthia II* **164/84,** 125–35.

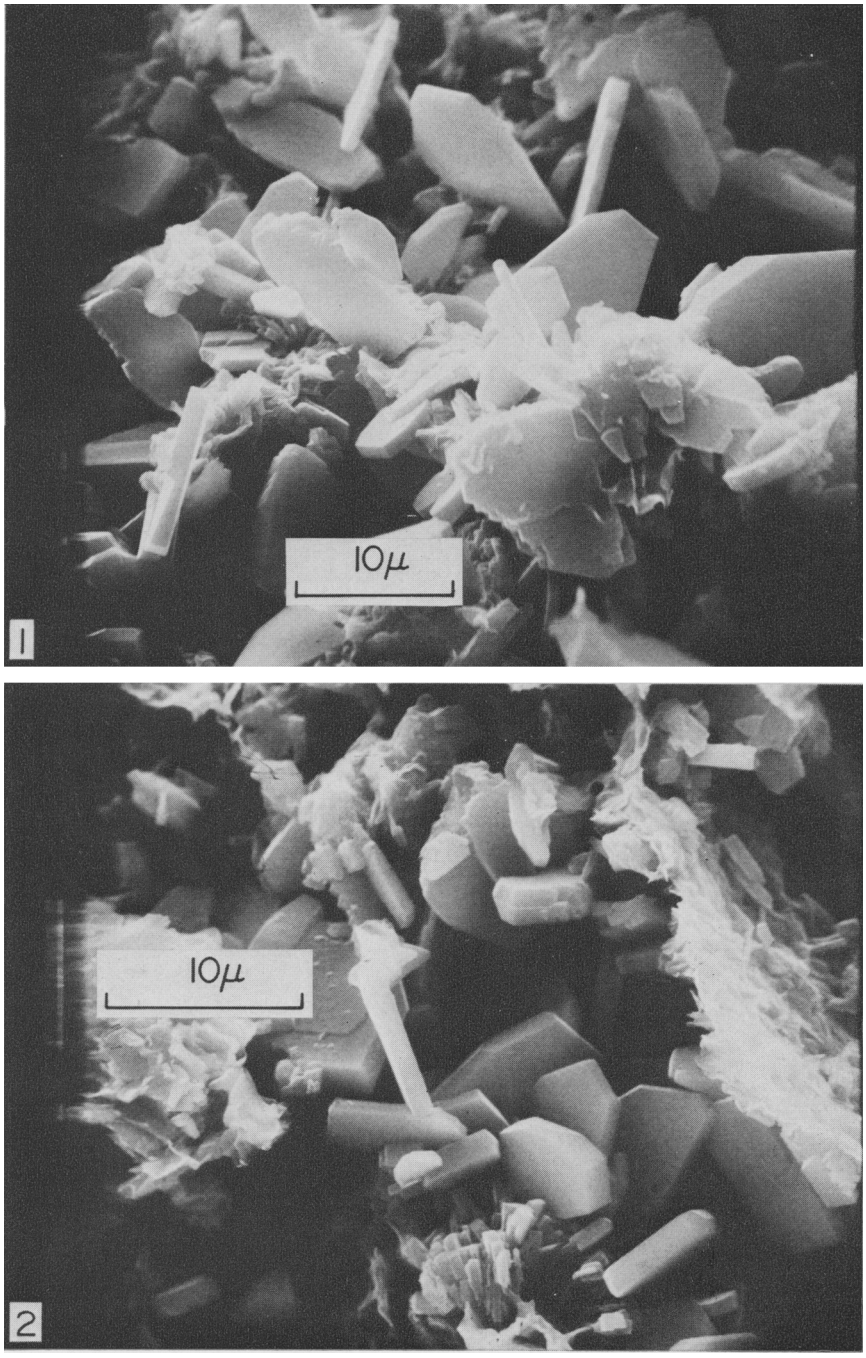

Fig. 1. Scanning electron micrograph of clinoptilolite from a lacustrine tuff near Castle Creek, Idaho. Note the characteristic monoclinic symmetry of the blades and laths, some of which are similar to the coffin-shape of megascopic heulandite that occurs in vugs in basalts. (Sample 25-5-25)

Fig. 2. Scanning electron micrograph of clinoptilolite from Castle Creek Idaho. Thin scales of montmorillonite are also present, although from X-ray diffraction analysis the sample is nearly pure clinoptilolite. (Sample 25-5-25)

https://doi.org/10.1346/CCMN.1976.0240101 Published online by Cambridge University Press

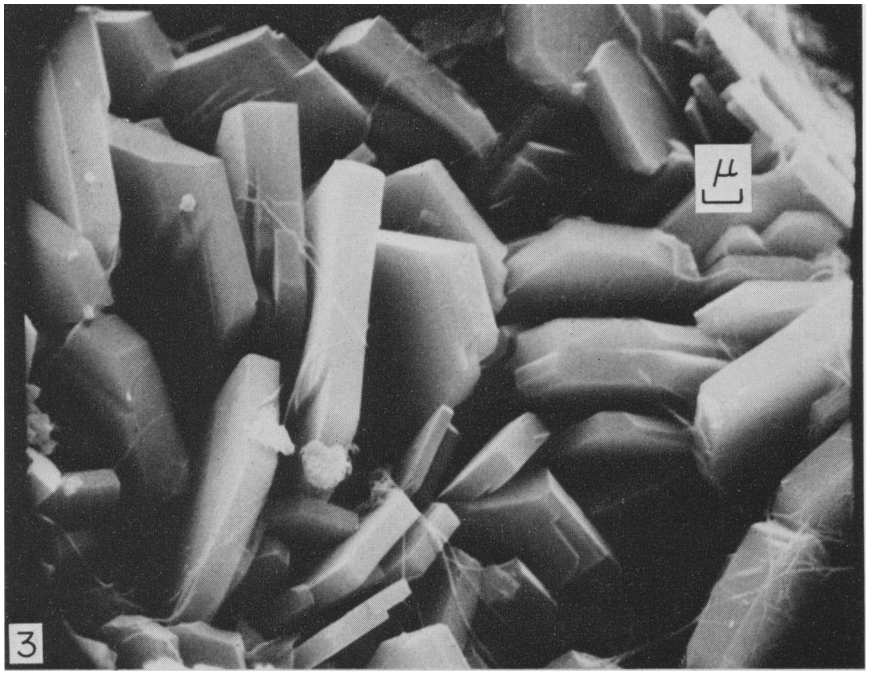

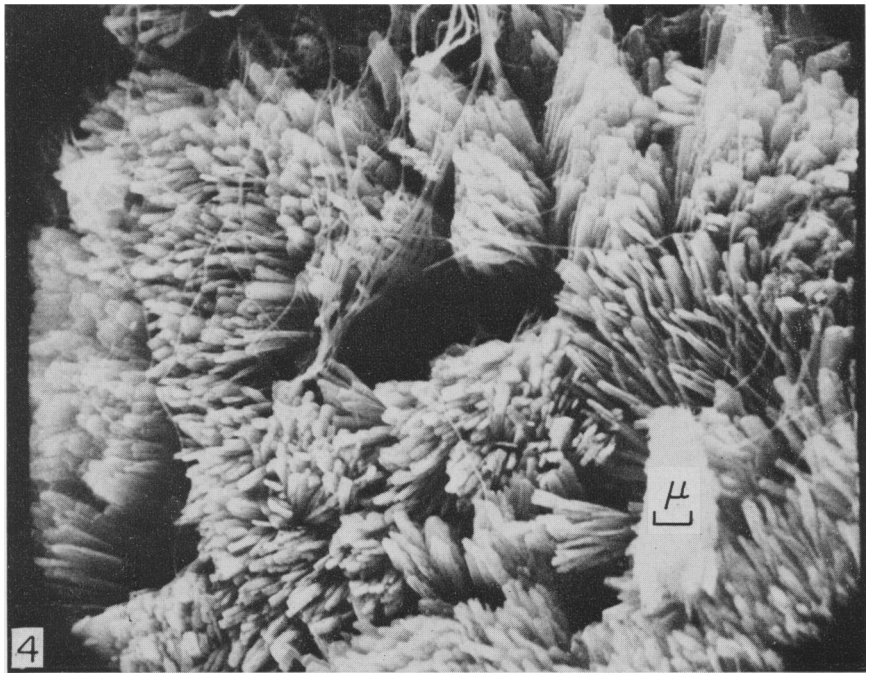

Fig. 3. Scanning electron micrograph of clinoptilolite from a lacustrine tuff near Hector, California, being mined by NL Industries. Filiform mordenite, detectable by X-ray diffraction analysis, crisscross among the clinoptilolite plates. (Sample 25-5-23)

Fig. 4. Scanning electron micrograph of clinoptilolite from a lacustrine tuff near Toponica, Serbia, Yugoslavia. The crystals resemble laths rather than plates but still display monoclinic symmetry. Mordenite fibers are also present. (Sample 25-13-19)

https://doi.org/10.1346/CCMN.1976.0240101 Published online by Cambridge University Press

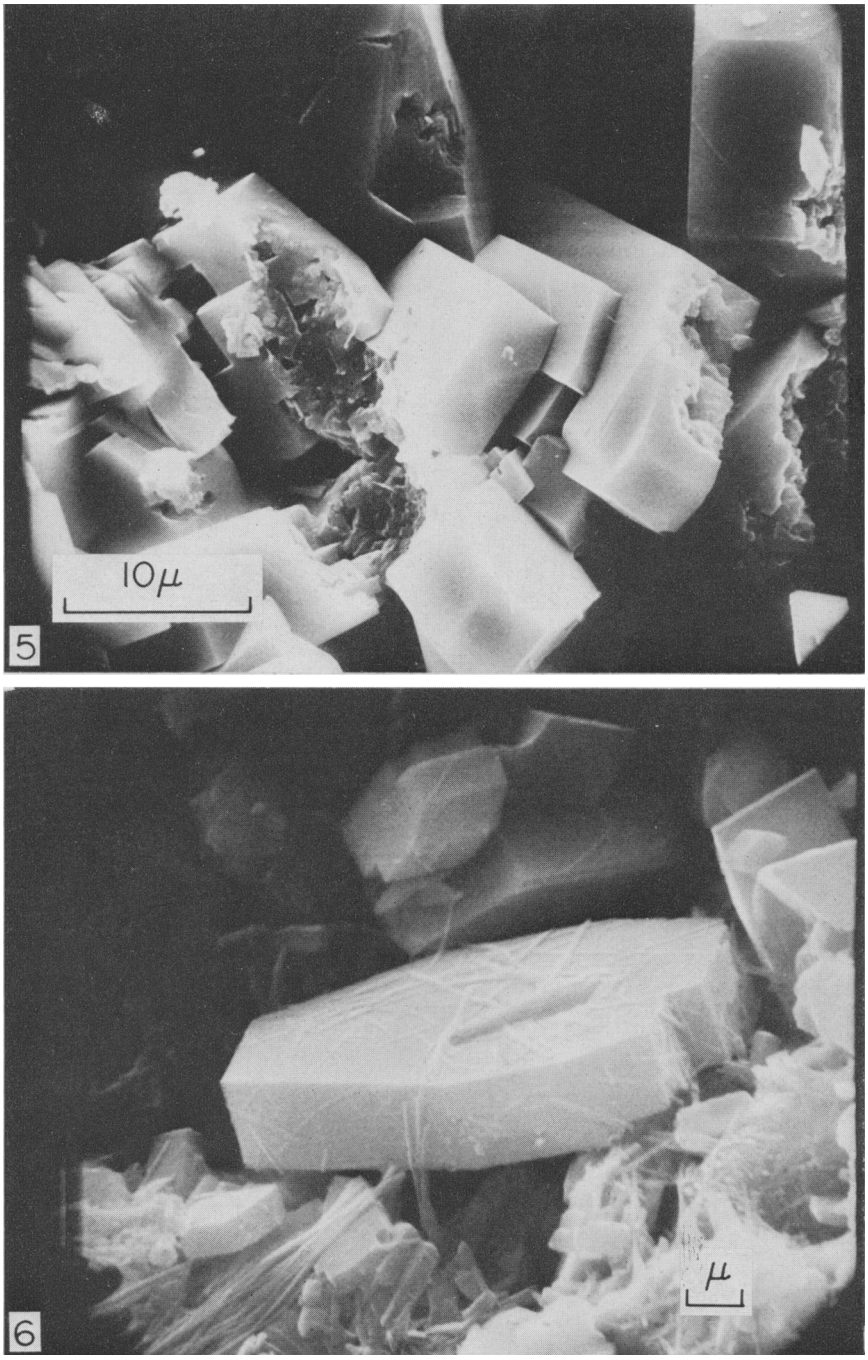

Fig. 5. Scanning electron micrograph of clinoptilolite from Hungry Valley, Nevada. The severely etched crystals are probably due to pore-water dissolution, after formation in a saline-lake environment. (Sample 42-41-20-1)

Fig. 6. Scanning electron micrograph of a coffin-shaped crystal of clinoptilolite from saline-lake tuff near Durkee, Oregon. The fibers coating the crystal are probably mordenite. (Sample 25-53-69)

https://doi.org/10.1346/CCMN.1976.0240101 Published online by Cambridge University Press

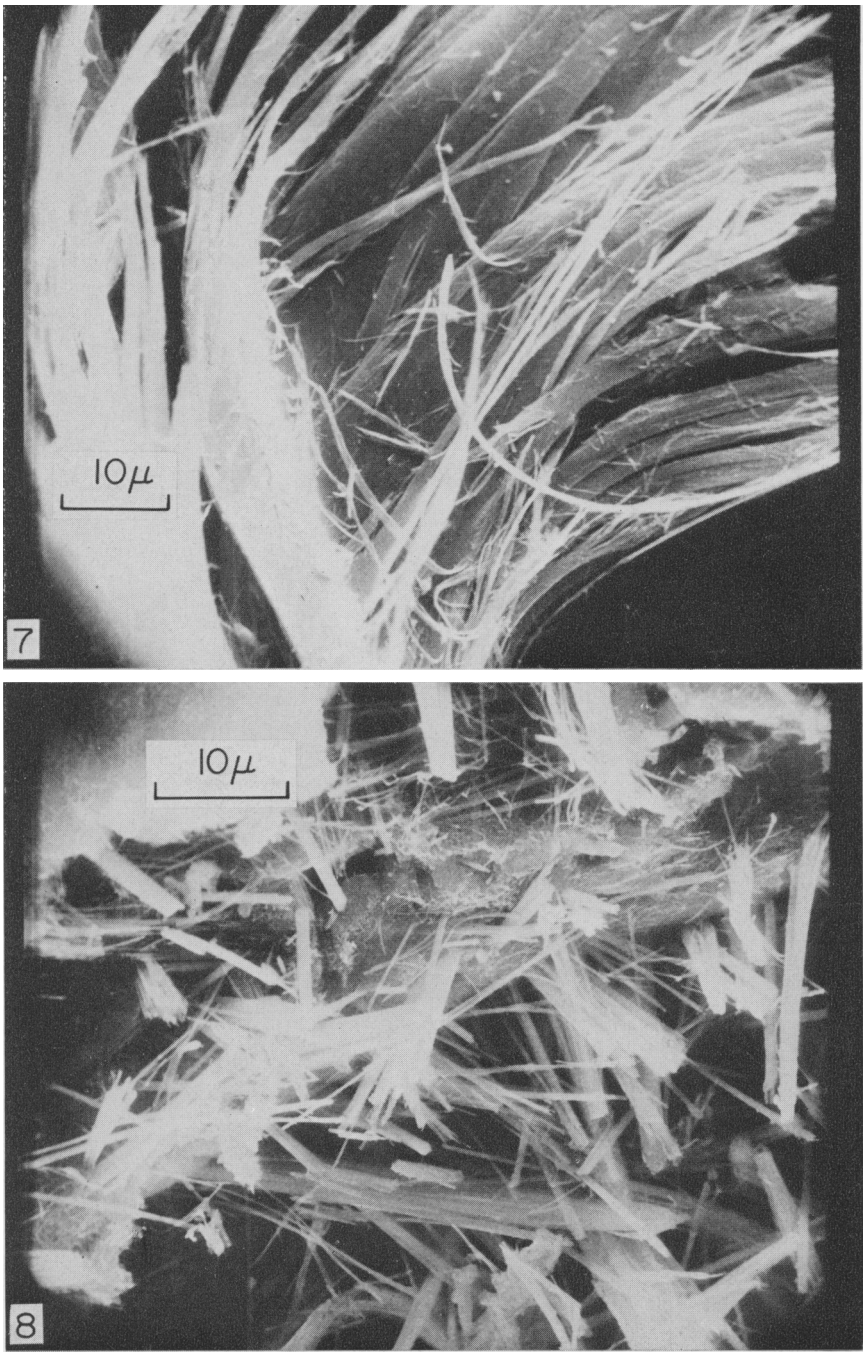

Fig. 7. Scanning electron micrograph of erionite from the type locality near Durkee, Oregon. The woolly fibers are several hundred microns long and split readily into fibrils less than 1μm in diameter. (Sample 25-43-161)

Fig. 8. Scanning electron micrograph of erionite needles from a saline-lake tuff near Eastgate, Nevada. The needles are 10–20 μm in length and about 1 μm thick. (Sample 42-60-66)

https://doi.org/10.1346/CCMN.1976.0240101 Published online by Cambridge University Press

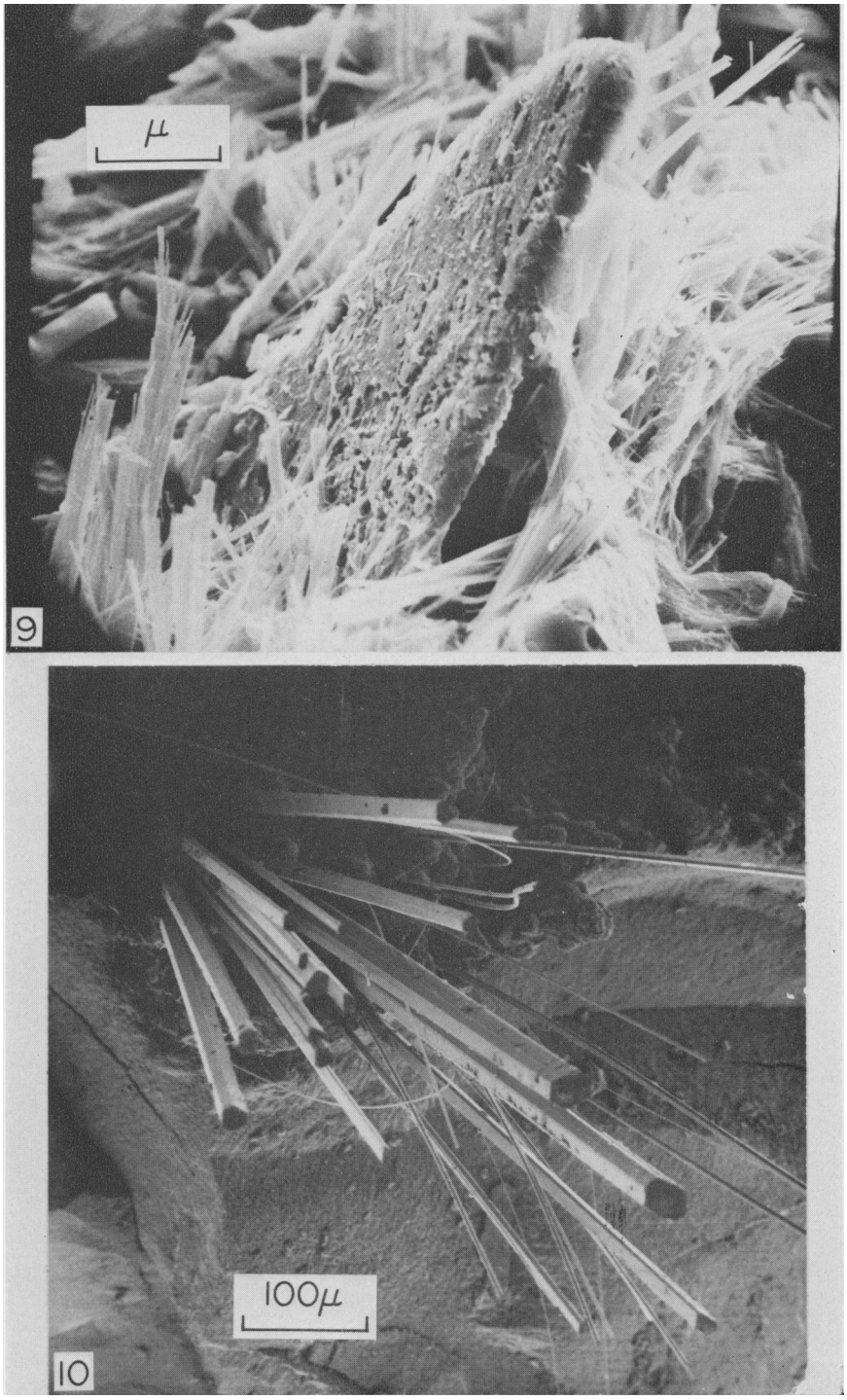

Fig. 9. Scanning electron micrograph of erionite and parent volcanic glass from a saline-lake tuff in Jersey Valley, Nevada, mined by Mobil Petroleum Corporation. The pitted nature of the glass shard is probably the result of arrested pore-water dissolution. (Sample 25-43-127)

Fig. 10. Scanning electron micrograph of megascopic erionite from a basalt cavity. The hexagonal symmetry is readily apparent. The rods are several hundred μm in length. (Fig. 4, Waltinger and Zirkl, 1974)

https://doi.org/10.1346/CCMN.1976.0240101 Published online by Cambridge University Press

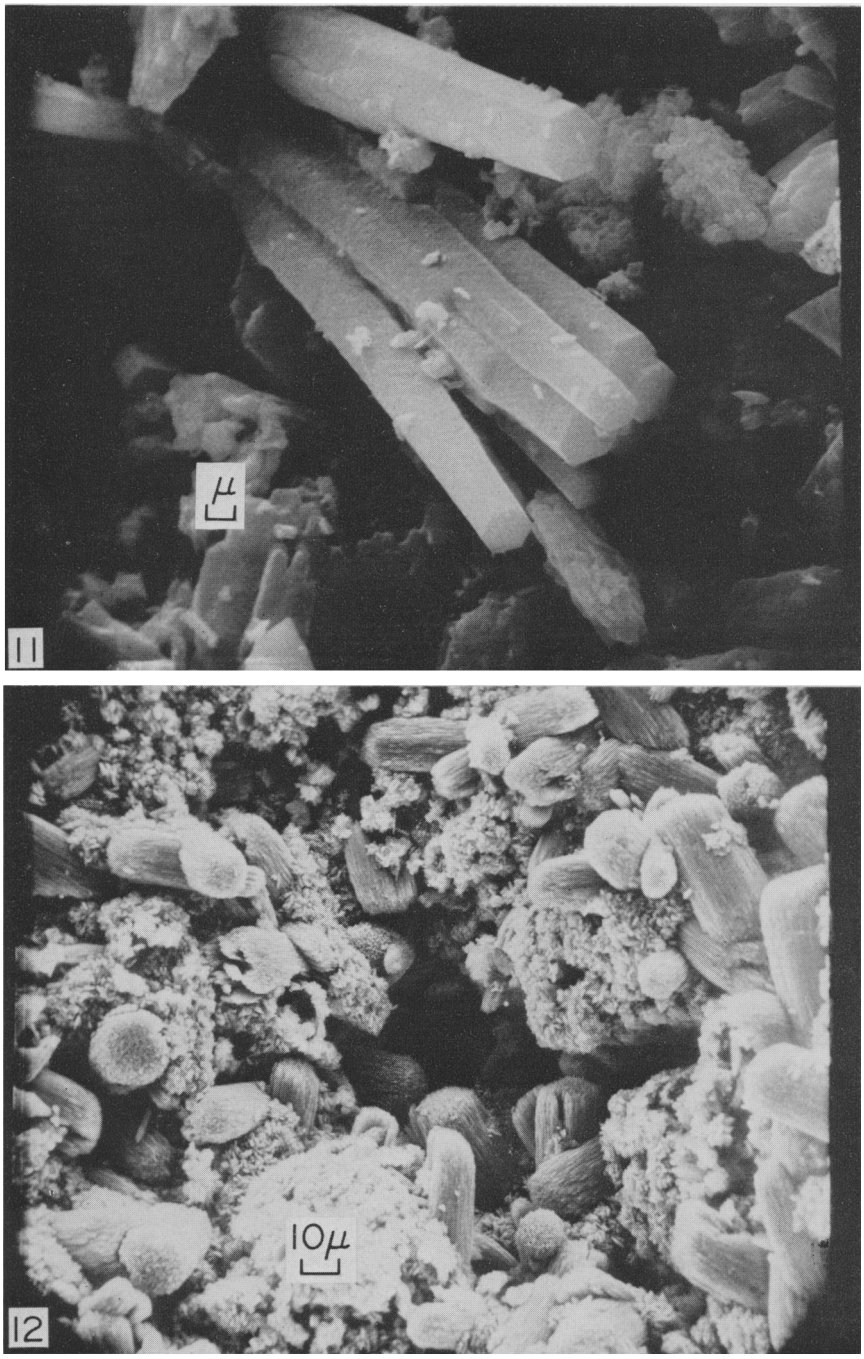

Fig. 11. Scanning electron micrograph of sedimentary erionite from a saline-lake tuff near Shoshone, California. Note the hexagonal symmetry of the rods and their similarity with the erionite shown in Fig. 10. (Sample 25-7-5)

Fig. 12. Scanning electron micrograph of bean-shaped bundles of erionite from a lacustrine tuff near Hector, California. The bundles are about 20 μm long and about 10 μm thick. (Sample 25-43-45)

https://doi.org/10.1346/CCMN.1976.0240101 Published online by Cambridge University Press

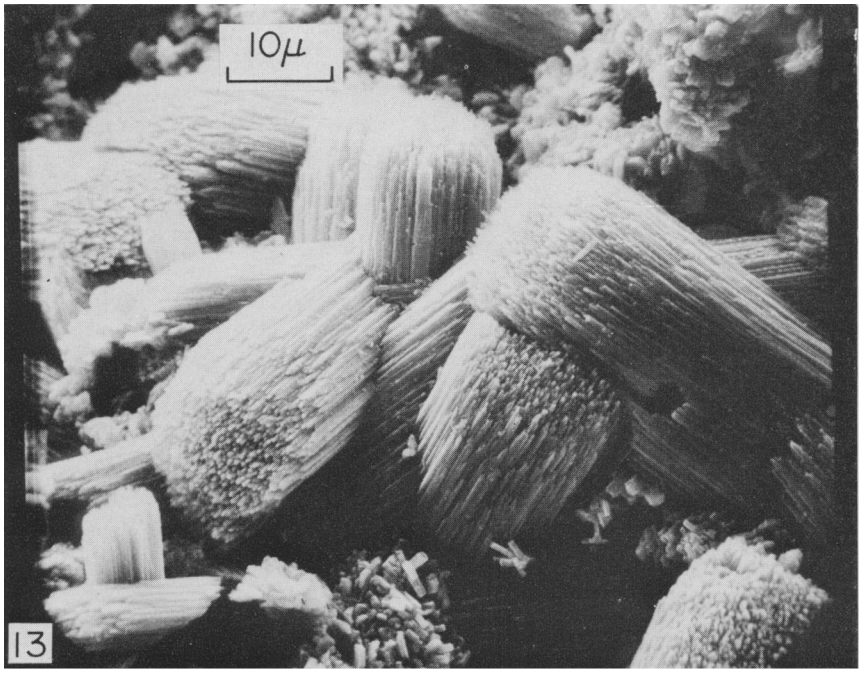

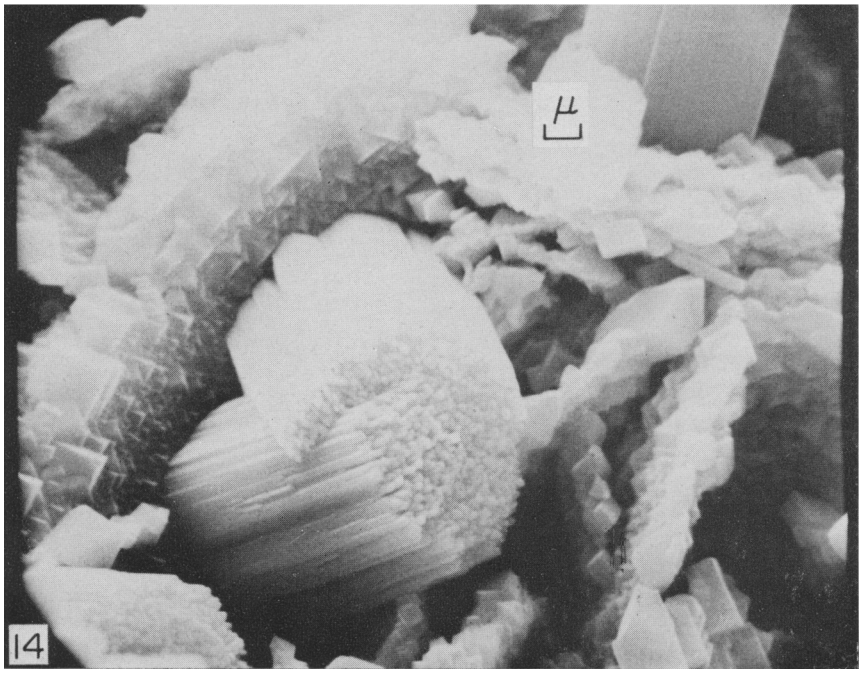

Fig. 13. Scanning electron micrograph of erionite from Hector, California, at higher magnification. The bundles consist of hundreds of individual needles, each about a half-micron thick. (Sample 25-43-45)

Fig. 14. Scanning electron micrograph of erionite bundles from a saline-lake tuff north of Bowie, Arizona. The bundles are surrounded by intergrowths of micron-size chabazite crystals. (Sample 25-43-152-1)

https://doi.org/10.1346/CCMN.1976.0240101 Published online by Cambridge University Press

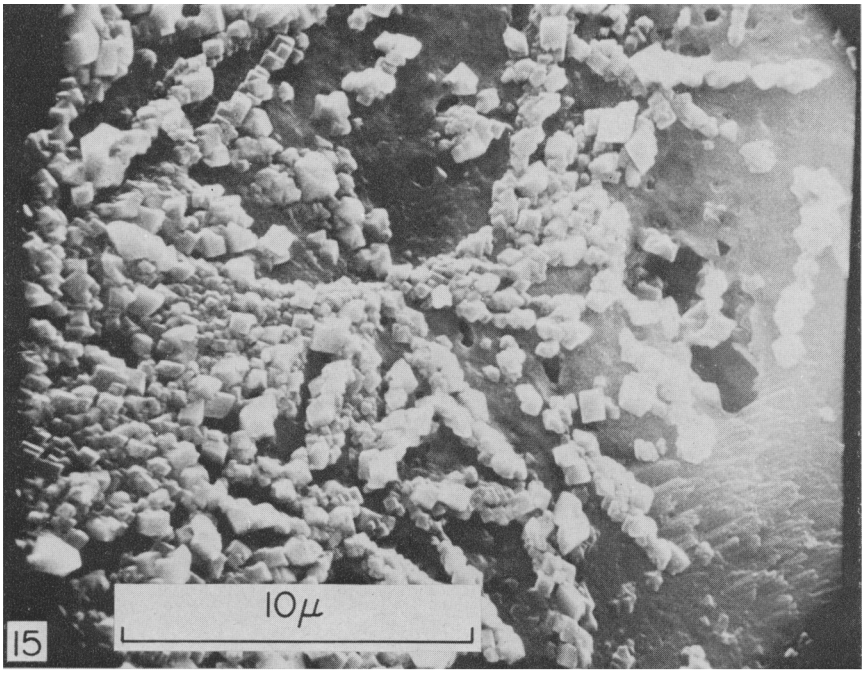

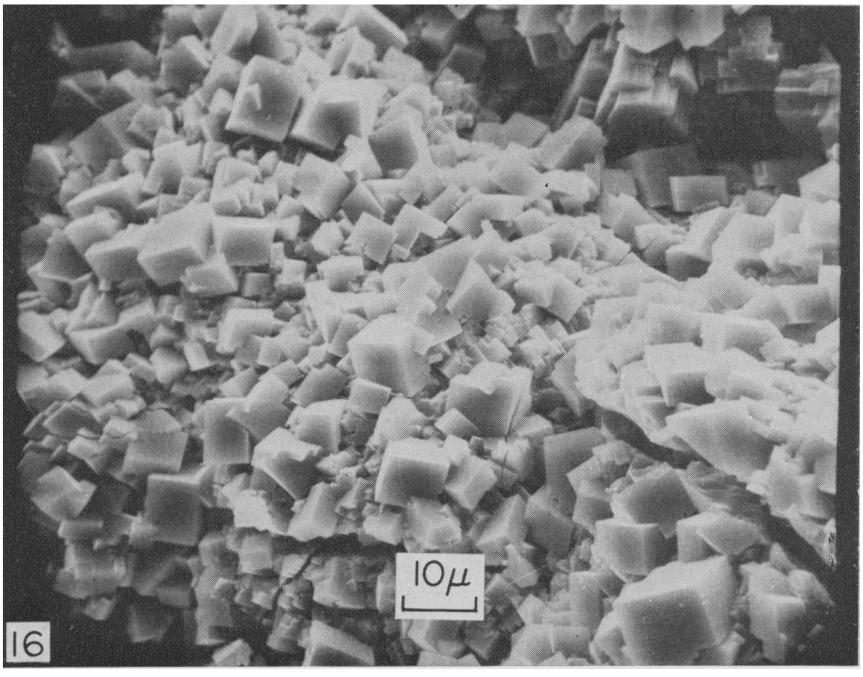

Fig. 15. Scanning electron micrograph of micron-size "cubes" or "rhombs" of chabazite from the Bowie, Arizona, zeolite deposit. The crystals commonly form polycrystalline crusts or strings of crystals as seen in the upper righthand corner of the figure. (Sample 25-43-152-2)

Fig. 16. Scanning electron micrograph of chabazite "cubes" or "rhombs" from a lacustrine tuff along Beaver Divide, Wyoming. The crystals are several microns in diameter and are commonly intergrown. (Sample 25-7-4)

https://doi.org/10.1346/CCMN.1976.0240101 Published online by Cambridge University Press

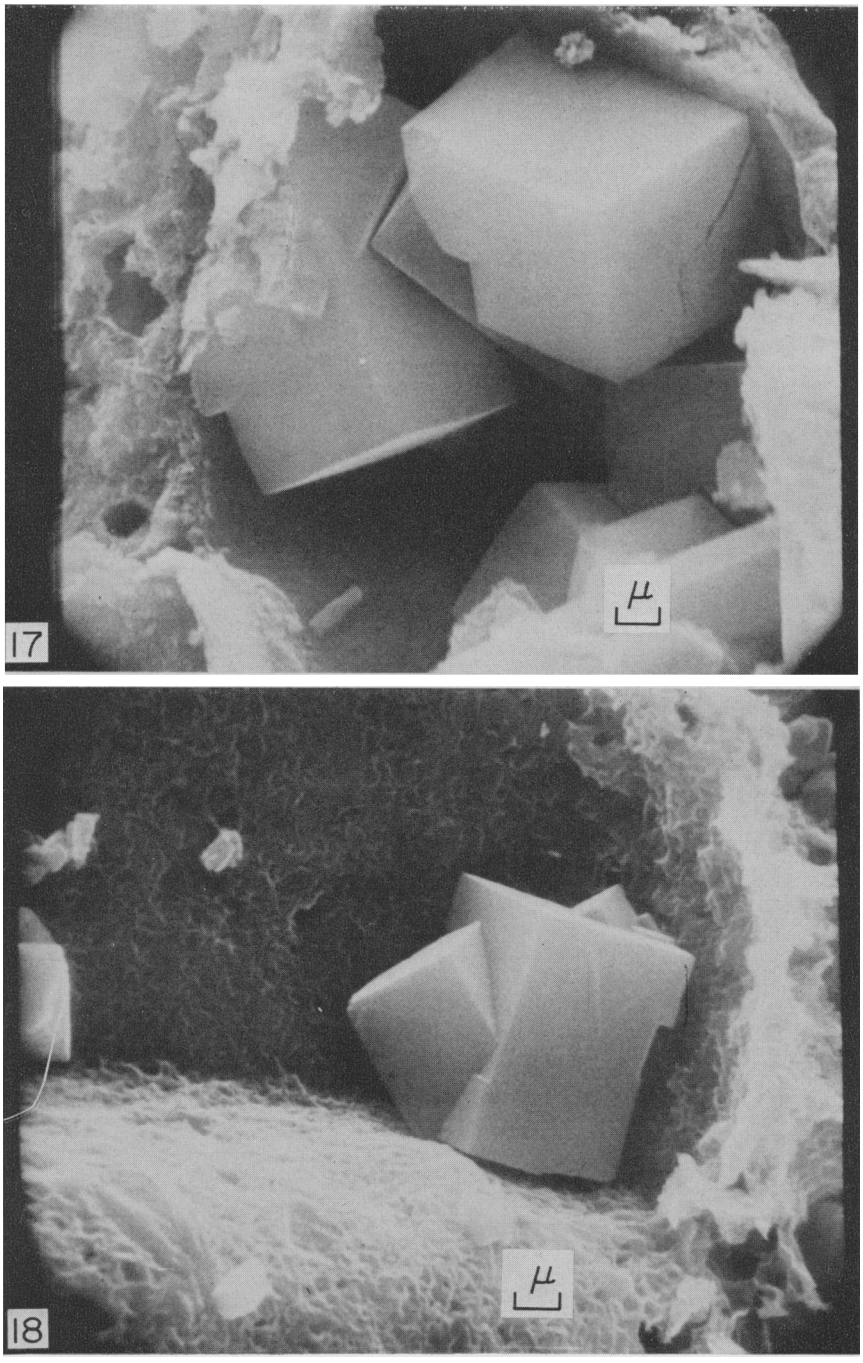

Fig. 17. Scanning electron micrograph of well-formed chabazite crystals from a marine tuff near Kruft, Germany, currently mined as a pozzolan. (Sample 42-51-4)

Fig. 18. Scanning electron micrograph of an isolated chabazite crystal in a saline-lake tuff near Durkee, Oregon. The surrounding matrix is probably montmorillonite. (Sample 25-53-128)

https://doi.org/10.1346/CCMN.1976.0240101 Published online by Cambridge University Press

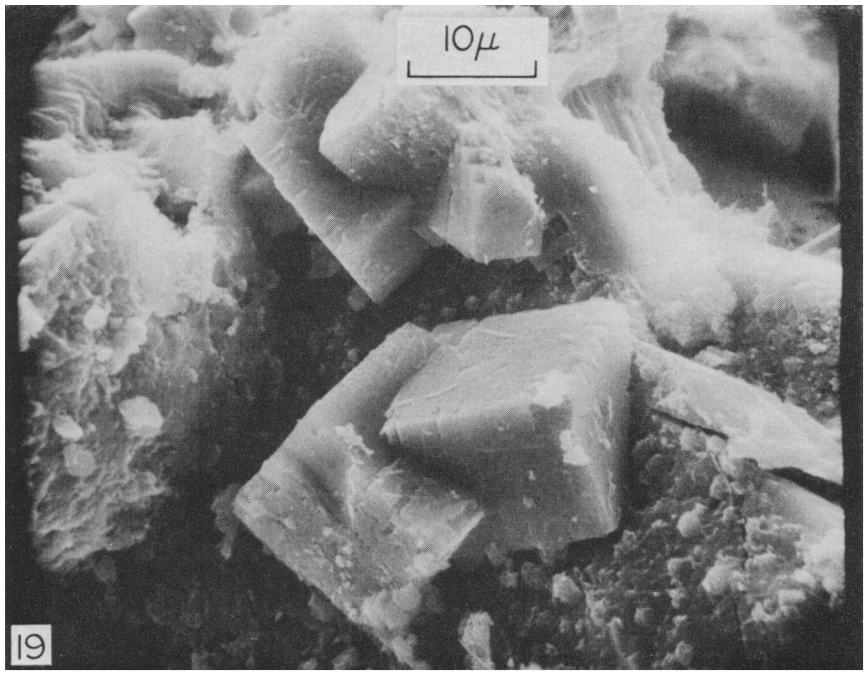

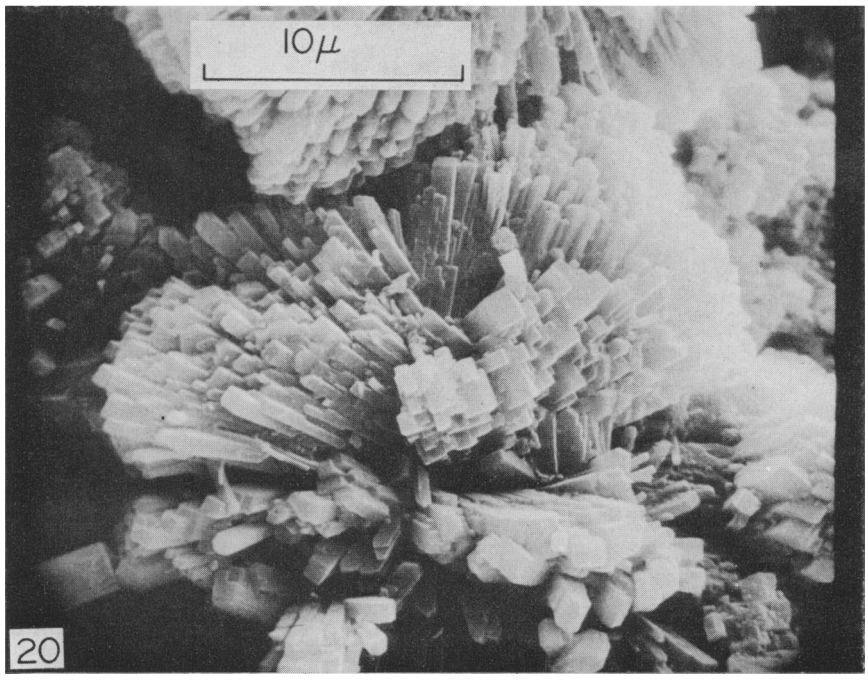

Fig. 19. Scanning electron micrograph of chabazite crystals, somewhat mottled in appearance, from a saline-lake tuff in the Reese River Valley, Nevada.

Fig. 20. Scanning electron micrograph of rosettes of phillipsite from saline-lake tuff in Pine Valley, Nevada. The prisms and laths are about 3–30 μm long and 0.3 to 3 μm thick. (Sample 25-7-6)

https://doi.org/10.1346/CCMN.1976.0240101 Published online by Cambridge University Press

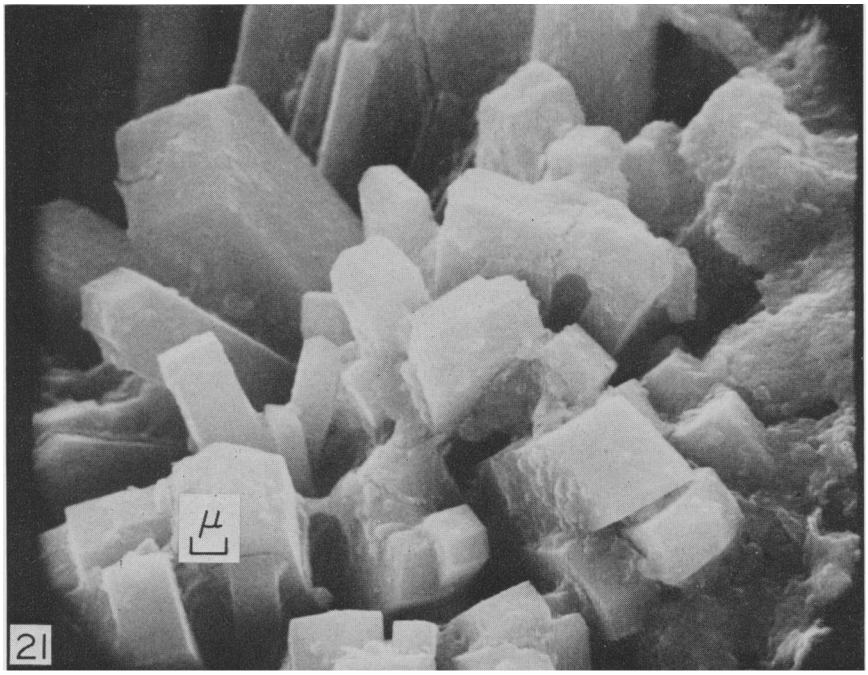

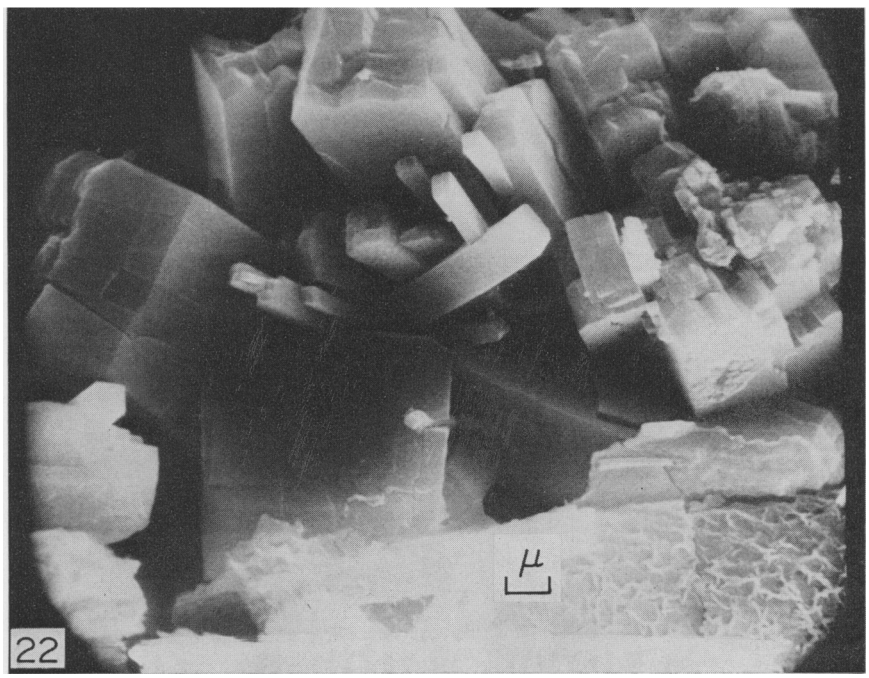

Fig. 21. Scanning electron micrograph of phillipsite prisms from Pine Valley, Nevada, displaying characteristic pseudo-orthorhombic symmetry. (Sample 25-7-6)

Fig. 22. Scanning electron micrograph of phillipsite prisms from a marine tuff near Naples, Italy (*Tufo giallo napolitano*). Note the "cracking" of many crystals along cleavage surfaces parallel to the axis of elongation. Montmorillonite is also present in this sample. (Sample 25-37-106)

https://doi.org/10.1346/CCMN.1976.0240101 Published online by Cambridge University Press

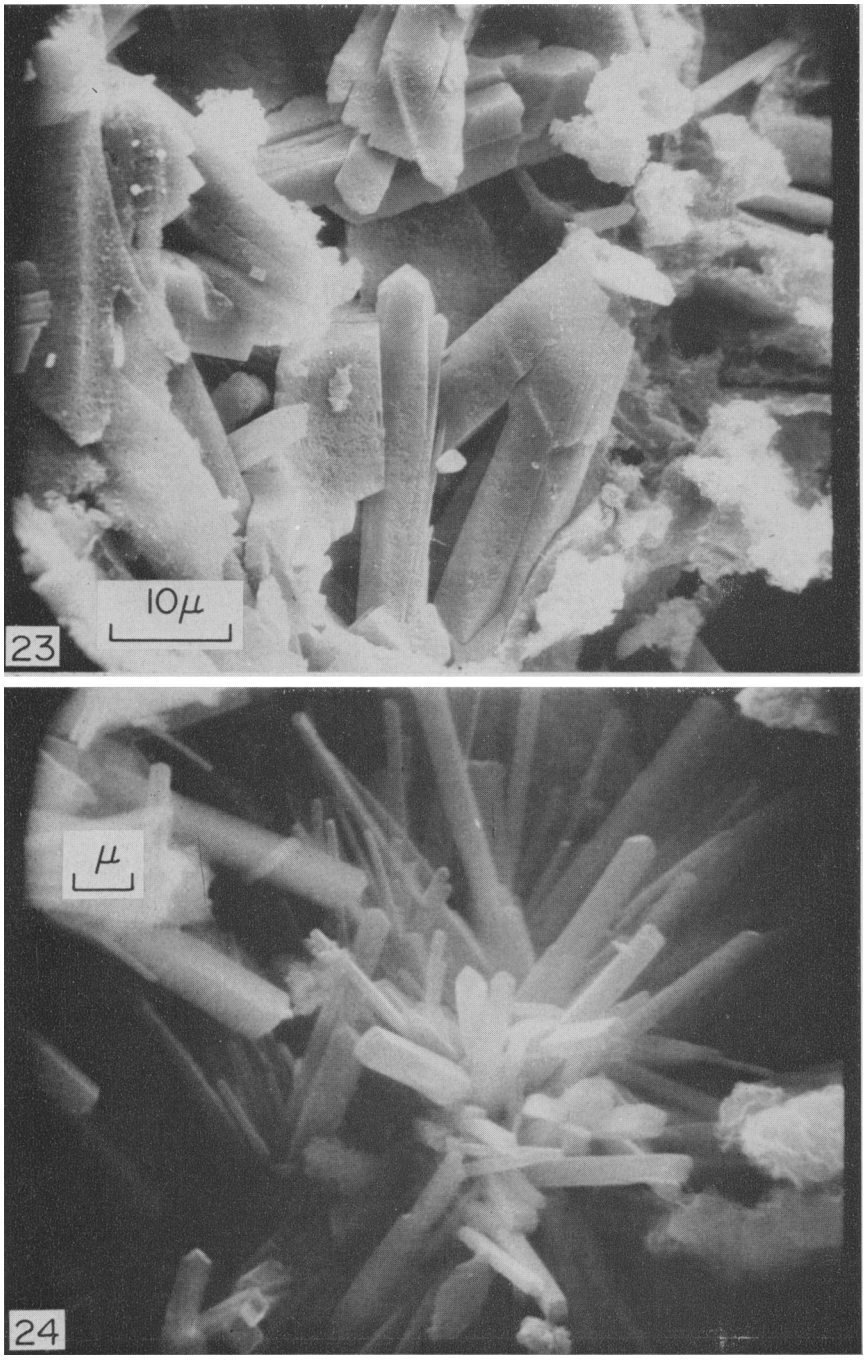

Fig. 23. Scanning electron micrograph of phillipsite laths and prisms from a saline-lake tuff near Kirkland, Arizona. Montmorillonite is also abundant in this sample. (Sample 25-7-7)
Fig. 24. Scanning electron micrograph of radiating rods of phillipsite in a marine tuff near Marino, Rome, Italy. (Sample 25-37-107)

https://doi.org/10.1346/CCMN.1976.0240101 Published online by Cambridge University Press

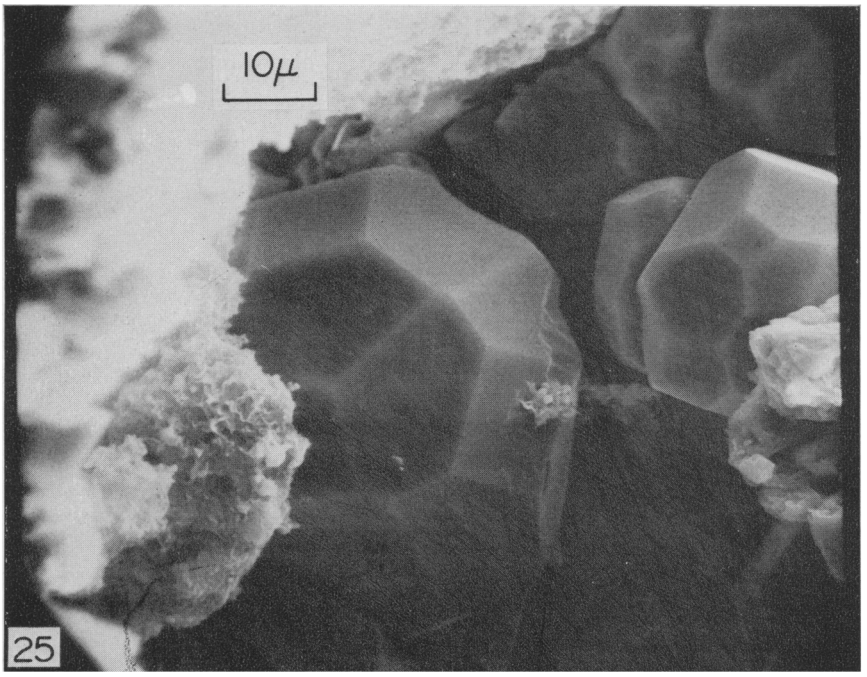

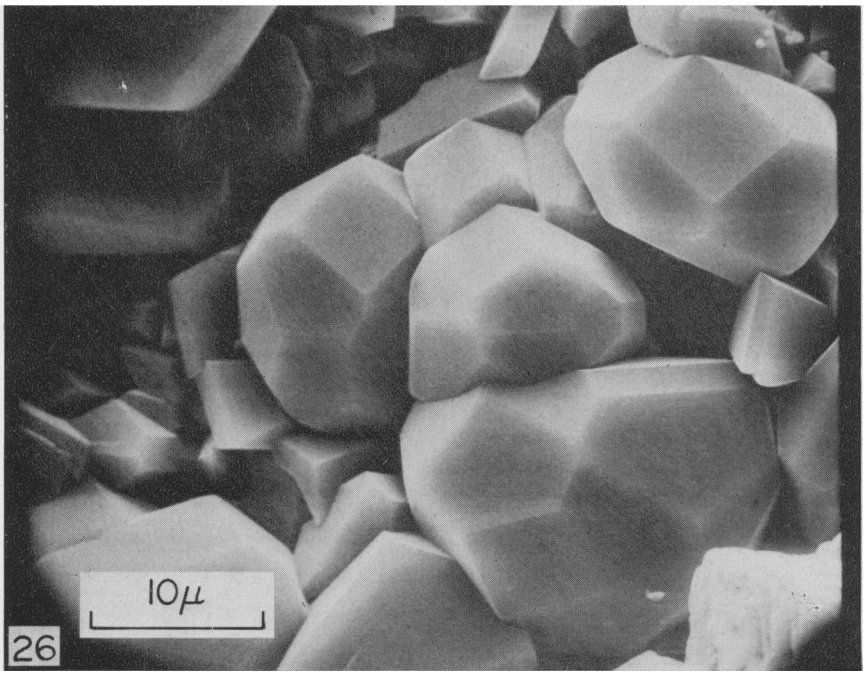

Fig. 25. Scanning electron micrograph of euhedral analcime from a marine tuff from Ischia, Italy. Note the characteristic cubo-octahedral and trapazohedral symmetry. (Sample 42-51-53)
Fig. 26. Scanning electron micrograph of an assemblage of analcime crystals from Ischia, Italy. Crystals range from 5 to 25 μm in size. (Sample 42-51-53)

https://doi.org/10.1346/CCMN.1976.0240101 Published online by Cambridge University Press

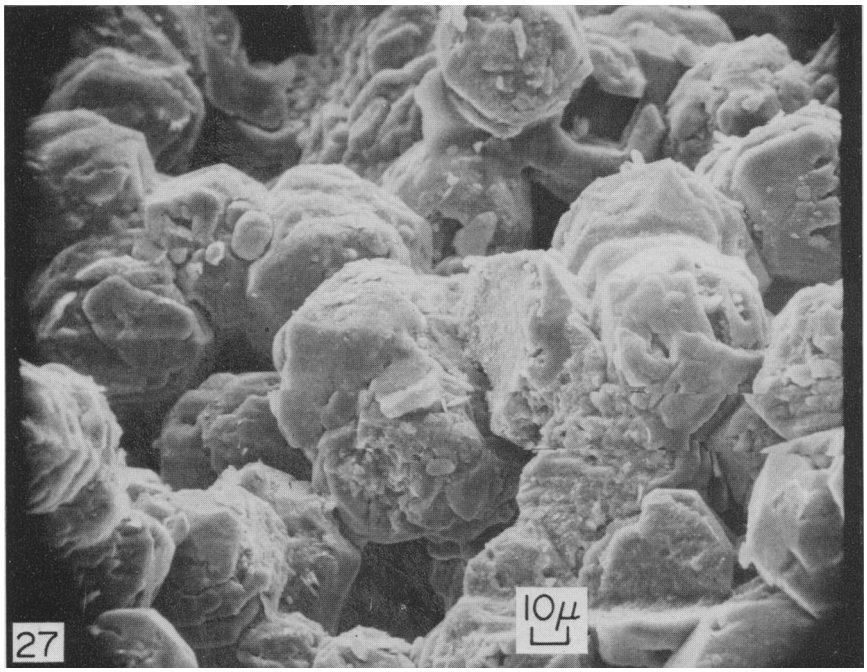

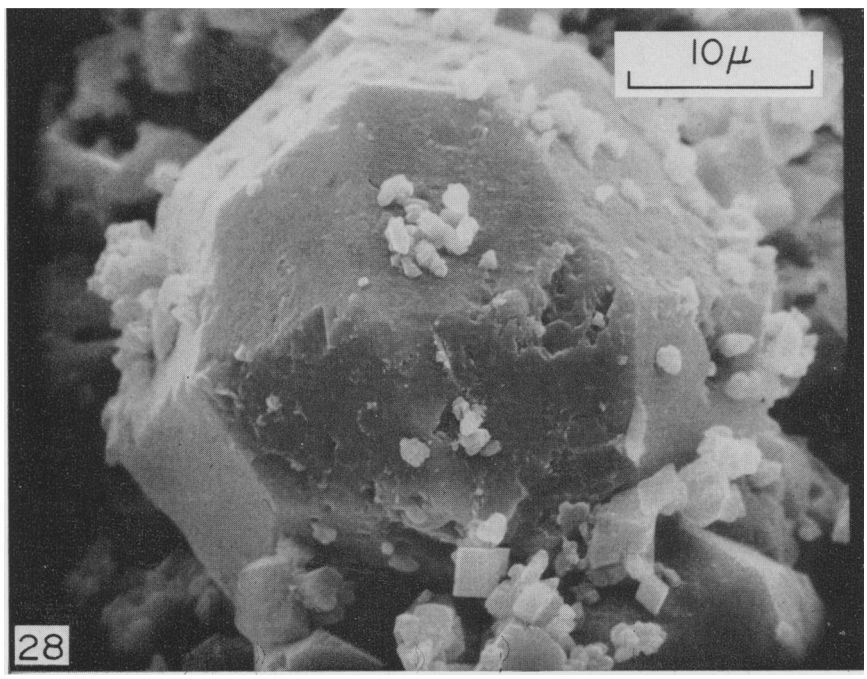

Fig. 27. Scanning electron micrograph of analcime crystals from a saline-lake tuff near Wikieup, Arizona. Subhedral crystals are coated with a probable ferruginous clay mineral. (Sample 25-53-6)
Fig. 28. Scanning electron micrograph of a well-formed analcime crystal from Wikieup, Arizona, about 30 μm in diameter. (Sample 25-53-6)

https://doi.org/10.1346/CCMN.1976.0240101 Published online by Cambridge University Press

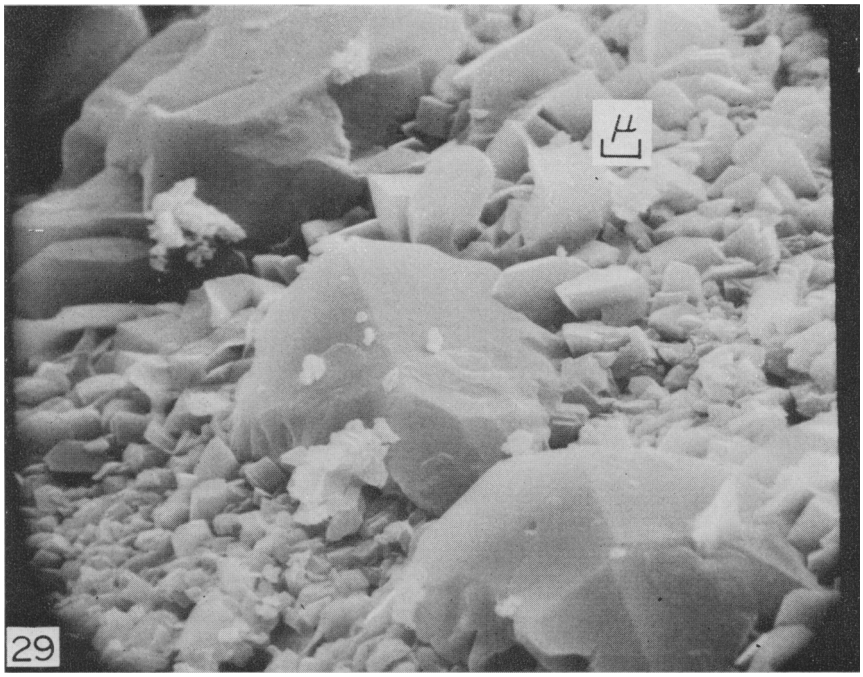

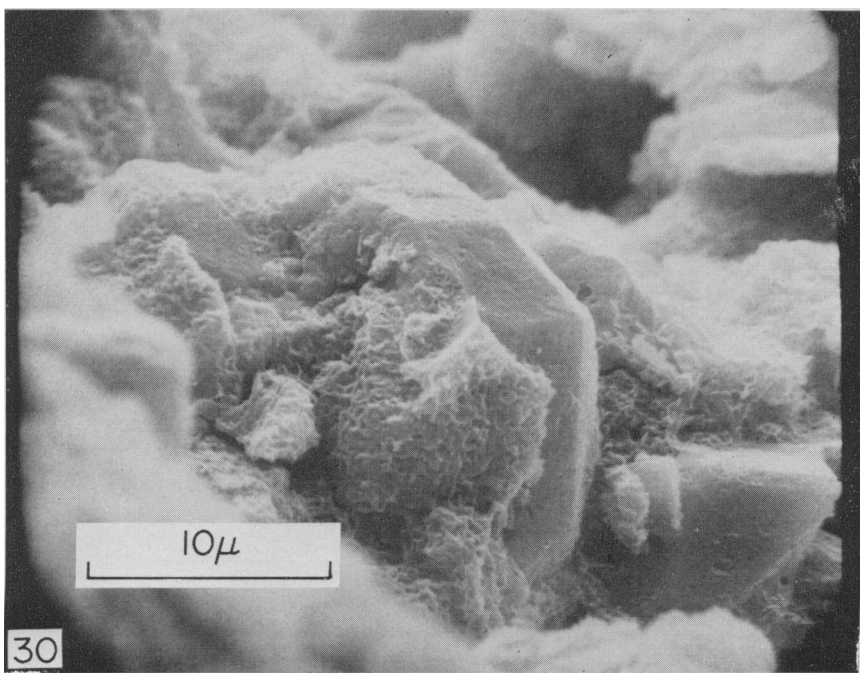

Fig. 29. Scanning electron micrograph of large analcime crystals in a matrix of micron-size crystals of potassium feldspar from a saline-lake tuff near Barstow, California. (Sample 25-43-136)
Fig. 30. Scanning electron micrograph of a large analcime crystal coated with montmorillonite from a lacustrine tuff near Tejupan, Oaxaca, Mexico. (Sample 42-47-18)

https://doi.org/10.1346/CCMN.1976.0240101 Published online by Cambridge University Press

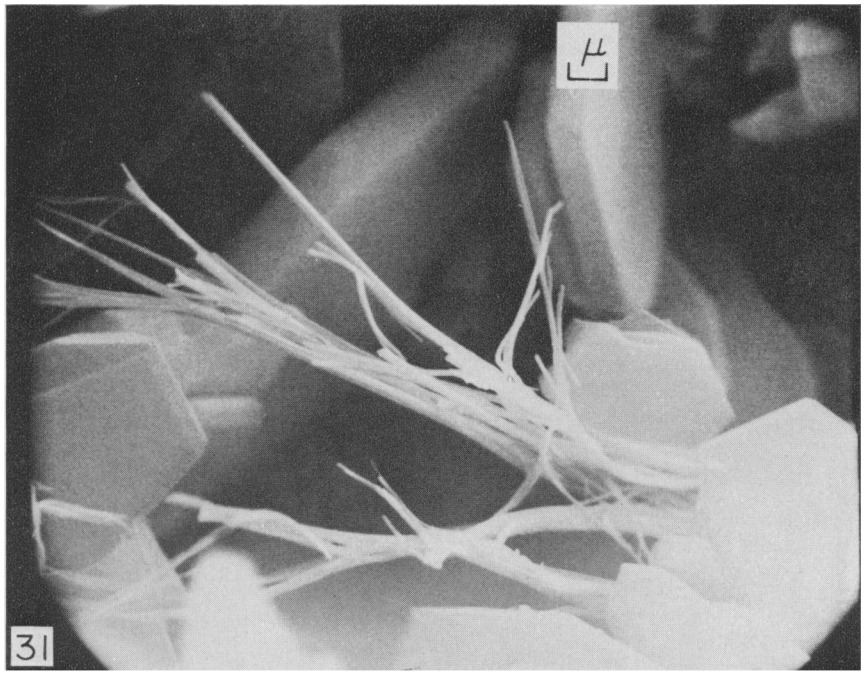

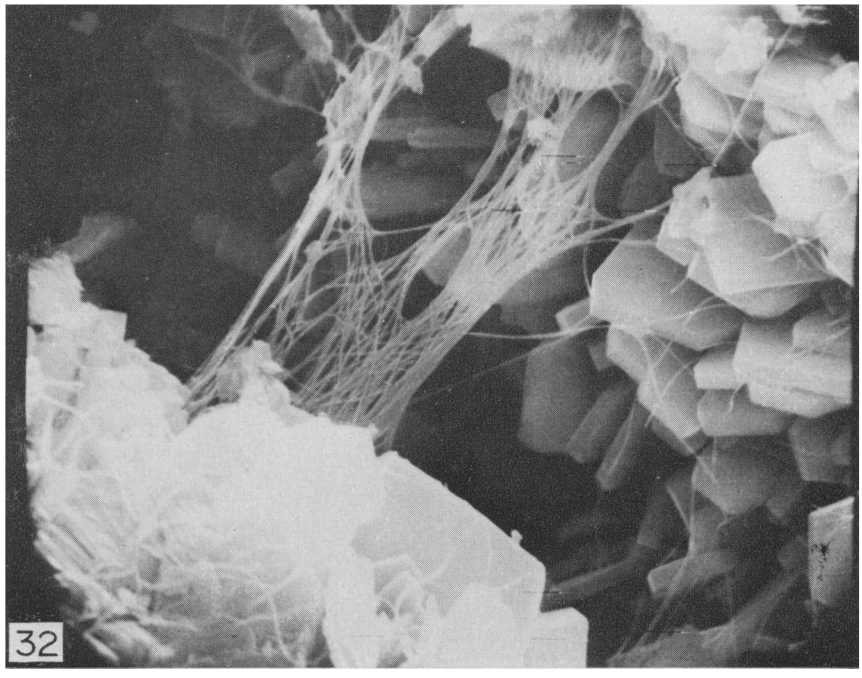

Fig. 31. Scanning electron micrograph of mordenite fibers and platy clinoptilolite from a lacustrine tuff near Castle Creek, Idaho. The fibers are from 0.1 to 0.2 μm in diameter and 10 to 20 μm in length. (Sample 25-5-25)

Fig. 32. Scanning electron micrograph of filiform mordenite bridging the gaps between clinoptilolite crystals in spider-web fashion in a lacustrine tuff near Hector, California. Individual fibrils are a few tenths of a micron in diameter. (Sample 25-5-23)

https://doi.org/10.1346/CCMN.1976.0240101 Published online by Cambridge University Press

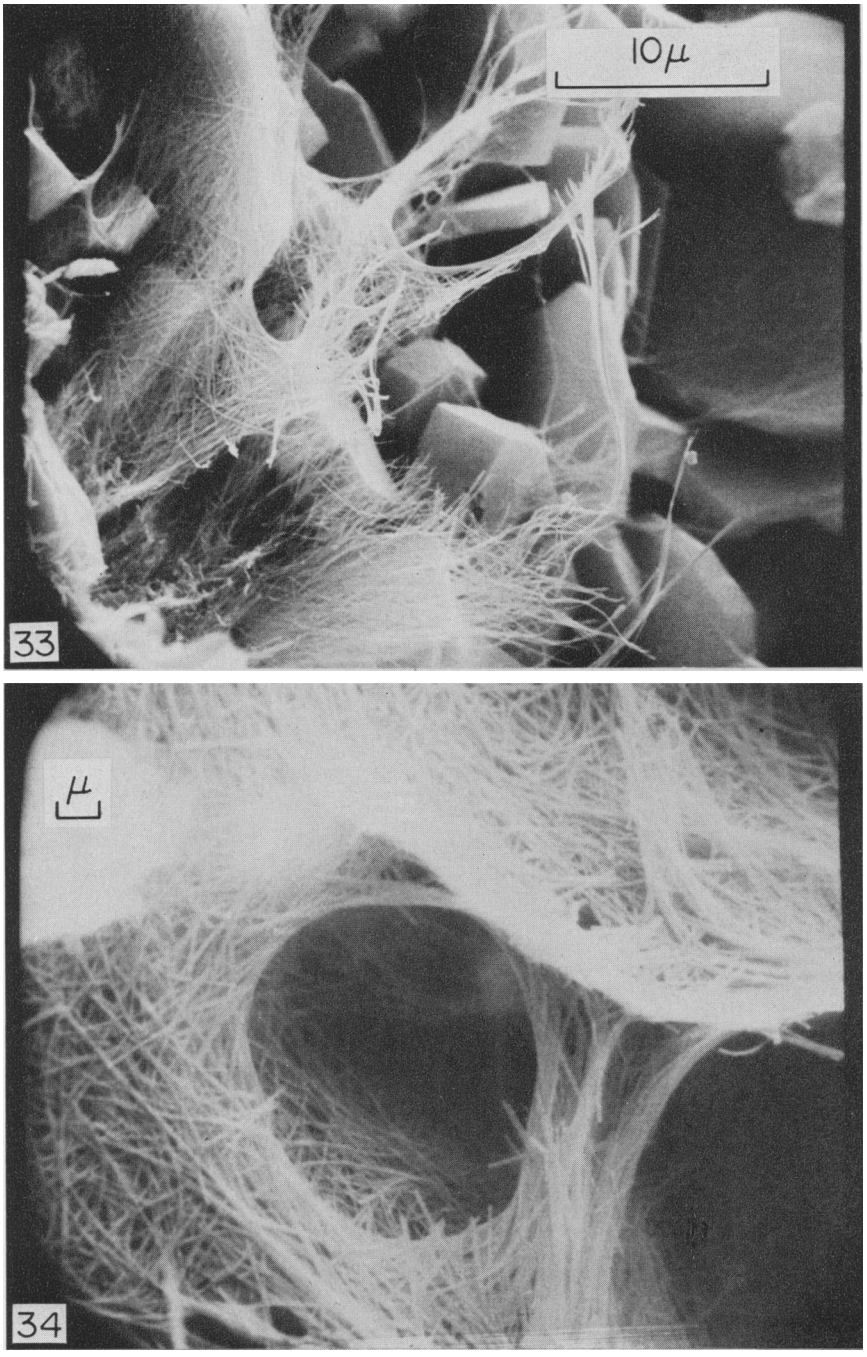

Fig. 33. Scanning electron micrograph of intertwined mordenite fibers with clinoptilolite from an ash-flow tuff near Monolith, California. This tuff has been mined by Monolith Portland Cement Company as a pozzolan. (Sample 25-5-5)

Fig. 34. Scanning electron micrograph of interlaced mordenite fibers in a monomineralic ash-flow tuff near Beatty, Nevada. Such "rats' nests" of fibers are not uncommon in many mordenite-rich tuffs. (Sample 42-41-11)

https://doi.org/10.1346/CCMN.1976.0240101 Published online by Cambridge University Press

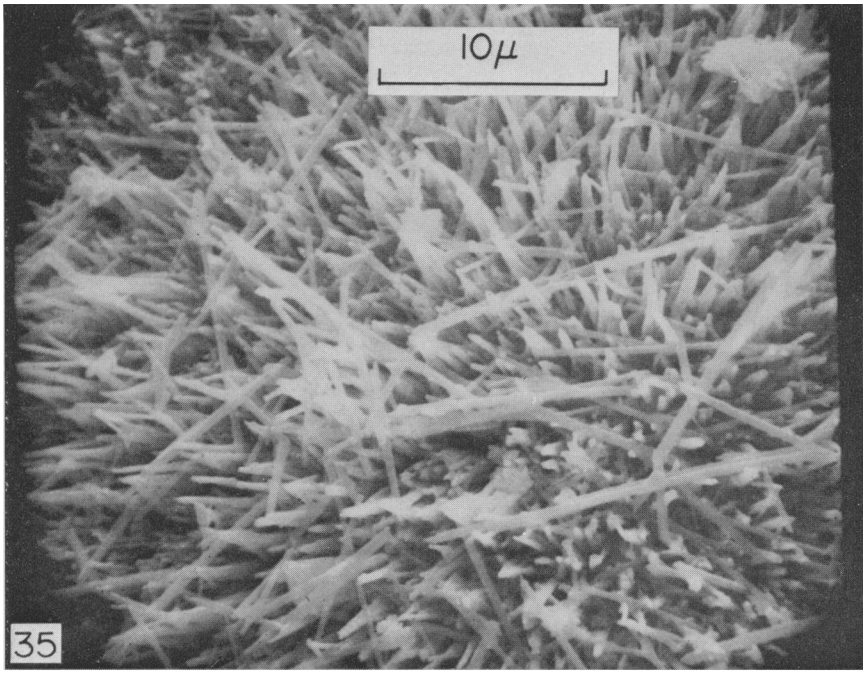

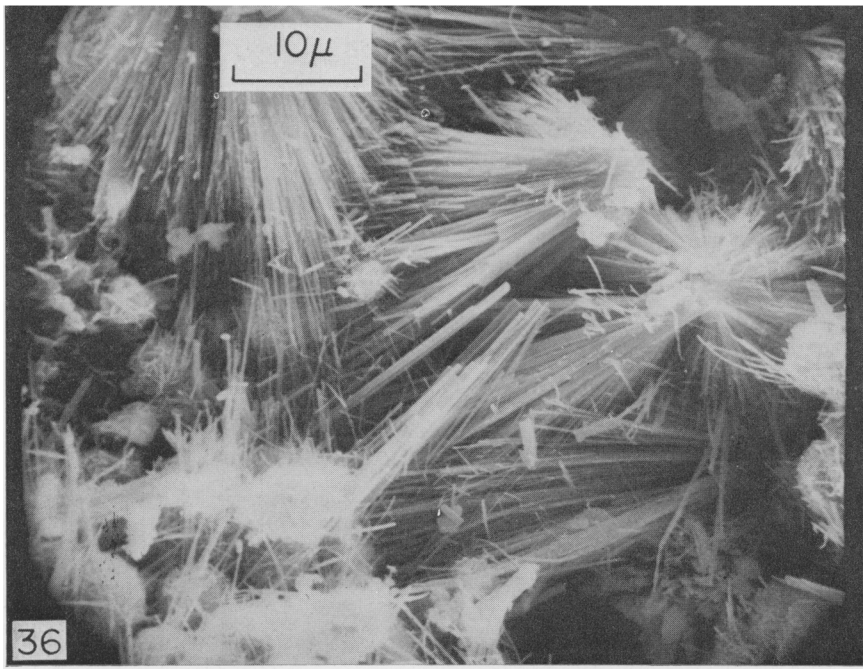

Fig. 35. Scanning electron micrograph of needle-shaped mordenite in a marine tuff near Pismo Beach, California. Individual needles are slightly less than one micron in diameter. (Sample 42-41-7)
Fig. 36. Scanning electron micrograph of bundles of radiating mordenite needles from a lacustrine tuff near Lovelock, Nevada. (Sample 42-60-69)

https://doi.org/10.1346/CCMN.1976.0240101 Published online by Cambridge University Press

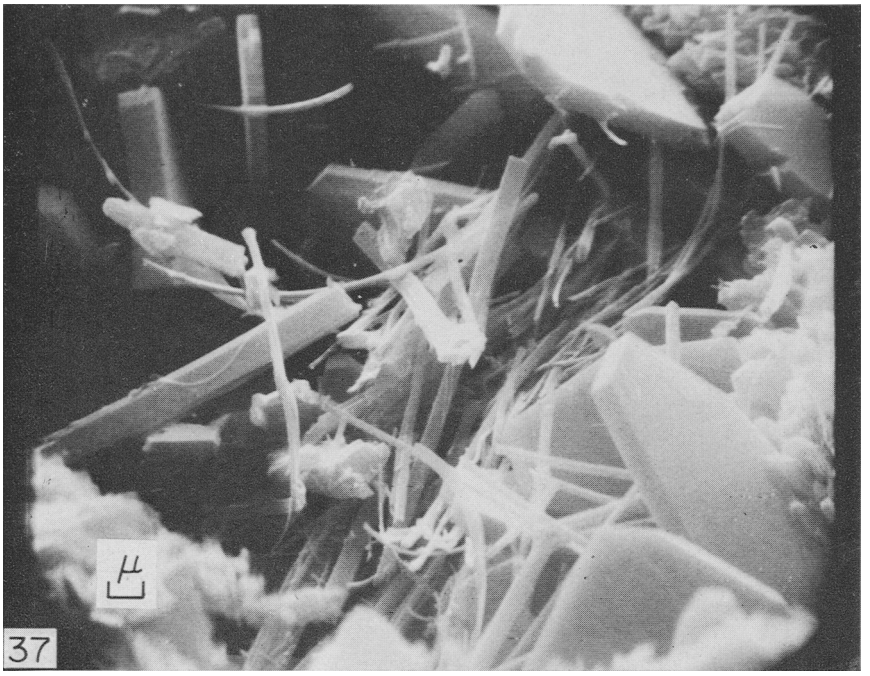

Fig. 37. Scanning electron micrograph of needles and fibers associated with clinoptilolite from a marine tuff near Dzegvi, Georgia, U.S.S.R. Although erionite or mordenite is suspected, neither can be identified from morphology alone, nor has either been detected in the sample by X-ray diffraction examination. (Sample 25-23-6)

https://doi.org/10.1346/CCMN.1976.0240101 Published online by Cambridge University Press